Fluorescence XAS using Ge PAD: Application to High-Temperature Superconducting Thin Film Single Crystals

H. Oyanagi,[1] A. Tsukada,[2,*] M. Naito,[2,*] N.L. Saini[3] and C. Zhang[1]

[1]*National Institute of Advanced Industrial Science and Technology, 1-1-1 Umezono, Tsukuba 305-8568, Japan*
[2]*NTT Basic Research Laboratories, 3-1 Morinosato-Wakamiya, Atsugi,Kanagawa 243-0198, Japan*
[3]*Universita di Roma "La Sapienza", P. le Aldo Moro 2, 00185 Roma, Italy*

Abstract. A Ge pixel array detector (PAD) with 100 segments was used in fluorescence x-ray absorption spectroscopy (XAS) study, probing local structure of high temperature superconducting thin film single crystals. Independent monitoring of individual pixel outputs allows real-time inspection of interference of substrates which has long been a major source of systematic error. By optimizing grazing-incidence angle and azimuthal orientation, smooth extended x-ray absorption fine structure (EXAFS) oscillations were obtained, demonstrating that strain effects can be studied using high-quality data for thin film single crystals grown by molecular beam epitaxy (MBE). The results of $(La,Sr)_2CuO_4$ thin film single crystals under strain are related to the strain dependence of the critical temperature of superconductivity.

Keywords: PAD, fluorescence x-ray absorption spectroscopy, thin film single crystal, high-temperature superconductor.
PACS: 61.10.Ht, 74.72.-h

INTRODUCTION

X-ray absorption spectroscopy (XAS) is a powerful local probe for high temperature supeconducting [1] (HTSC) cuprates. Previous works revealed that the local displacement of oxygens is intimately related to charge-lattice inhomogeneity [2] as carriers are doped, indicating the important role of electron-lattice interaction in the pairing mechanism. Isotope and strain (pressure) effects are considered as direct experiments that establish the role of lattice in HTSC. Under epitaxial strain, *T*-$(La,Sr)_2CuO_4$ (LSCO) thin film single crystals exhibit significant strain dependence of the superconducting critical temperature and metallic transport properties. We report that the use of a novel approach in x-ray detector, pixel array detector (PAD) successfully removes artifacts due to substrates providing high-qaulity XAS spectra [3].

PAD AND ELECTRONICS

The PAD used in this work consists of 10 x 10 array of germanium pixel (4.7 mm x 4.7 mm) with thickness t = 5 mm. Each pixel output is fed into a separate analog preamplifier board [4]. Preamplifier output for each channel is fed into one of linear input channels of analog-digital hybrid CAMAC module. A double width CAMCAC module contains 8 linear amplifiers, 32 single channel analyzers (SCAs), counters, memories, CAMAC bus interfaces and module control circuits. It has a 6th order Gaussian filer. Amplifier gain is adjustable between 25 and 200 and time constant is selectable from 0.5 μs, 10 μs and 3 μs. The resolution of LLD and SCA window width are 12 bits and 8 bits, respectively. Each SCA channel has a 24 bits counter and four independent memories. Sample (10 mm x 10 mm) is mounted on an aluminum holder and attached to a closed-cycle helium refrigerator which rotates on a high precision goniometer (Huber 420) to change the incidence angle.

XAS EXPERIMENT

The fluorescence signal is recorded over a cone-like solid angle perpendicular to the incidence beam away from scattering plane. This arrangement was used to measure EXAFS with the electric field vector ***E*** parallel with the *ab* plane (***E***//*ab*), while a sample is rotated by 90 degrees for probing along the *c*-axis (***E***//*c*).[2] Thin films of LSCO single crystal were grown in a molecular-beam epitaxy (MBE) chamber from metal sources using multiple electron-gun evaporators with accurate stoichiometry control of the atomic beam fluxes [5]. The samples were grown on

$LaSrAlO_4$ (LSAO) and $SrTiO_3$ (STO) substrates (10 mm x 10 mm).

Fluorescence yield spectra were obtained by integrating 100 channels giving a total count of 2.4 x 10^7 counts per data point. Each data point was integrated for four seconds and five independent scans were repeated to minimize systematic error. Figure 1 shows raw Cu K_α fluorescence yield as a function of photon energy measured for 100 nm thick $(La,Sr)_2CuO_4$ grown on $LaSrAlO_4$ with θ= 10 deg., θ= 5 deg., and θ= 1 deg. One can see that with the decrease of incidence angle, the effect of substrate diffractions is reduced and with θ= 1 deg., the artifact is not observed

RESULTS AND DISCUSSION

In Fig. 1, sharp peaks (artifacts due to standing waves) are evident in the EXAFS data around 10 $Å^{-1}$ and 14 $Å^{-1}$ with θ= 5 deg. (b) and θ= 10 deg. (a), respectively. As shown in the same plot with an expanded vertical scale, artifacts become less clear as the incidence angle is decreased and with θ= 1 deg. (a), most of diffraction effects disappear. The results demonstrate that grazing incidence geometry dramatically suppresses the effect from substrate. The geometry is further optimized by azimuthal rotation of the sample, monitoring PAD outputs as photon energy is scanned. Figure 1 shows the raw fluorescence yield spectra after normalizing by incidence beam intensity.

In Fig. 2a, the extracted EXAFS oscillations for LSCO/LSAO taken at 300 K are shown. One can find that the data taken without using grazing-incidence angle contain serious artifacts. Comparing the expanded scale data (Fig. 2b), the effect of incidence angle is obvious. Because of a lattice mismatch between LSCO and LSAO, thin film single crystals are compressively strained. In contrast to LSCO/LSAO, sample grown on $SrTiO_3$ (STO), LSCO/STO is under tensile strain. The critical temperature of superconductivity (T_c) under compressive and tensile strain are 43.4 K (+11% increase) and 19.0 K (-51% decrease), respectively. Although the magnitude of strain is almost the same for the two cases (compressive and tensile), T_c suppression under tensile strain is remarkable.

Individual EXAFS data (k < 18 $Å^{-1}$) for the nearest neighbor (NN) Cu-O_p (in-plane oxygen) and next-nearest neighbor (NNN) Cu-Cu correlations are filtered and curve fitted in k-space using a single scattering formula. Theory curves are calculated from a single scattering formula and theoretical phase shift functions using FEFF7 [6].

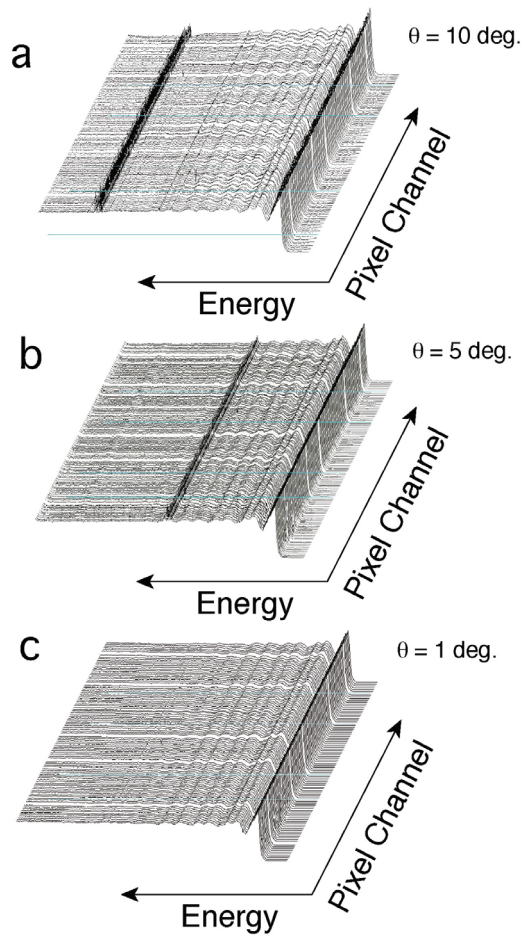

FIGURE 1. Fluorescence yield spectra of $(La,Sr)_2CuO_4$ thin film single crystal.

Structural parameters such as the in-plane Cu-O_p distance $R_{Cu\text{-}Op}$ and mean-square relative displacement of oxygens $\sigma^2_{Cu\text{-}Op}$ relative to copper ions are determined by least-squares curve-fitting in k-space. The determined $R_{Cu\text{-}Op}$ values for thin film LSCO/LSAO and LSCO/STO are 1.88 $\pm$ 0.01 Å and 1.90 $\pm$ 0.01 Å, respectively, in agreement with the crystallographic values, $a_0/2$ determined by x-ray diffraction patterns. Since the $R_{Cu\text{-}Op}$ in bulk single crystal is 1.89 $\pm$ 0.01 Å, the static local oxygen displacement within the CuO_2 plane, $\Delta R_{Cu\text{-}Op}/R_{Cu\text{-}Op}$ is about 5 x 10^{-3}. Why such a small shift of oxygen position significantly supresses T_c is an interesting question.

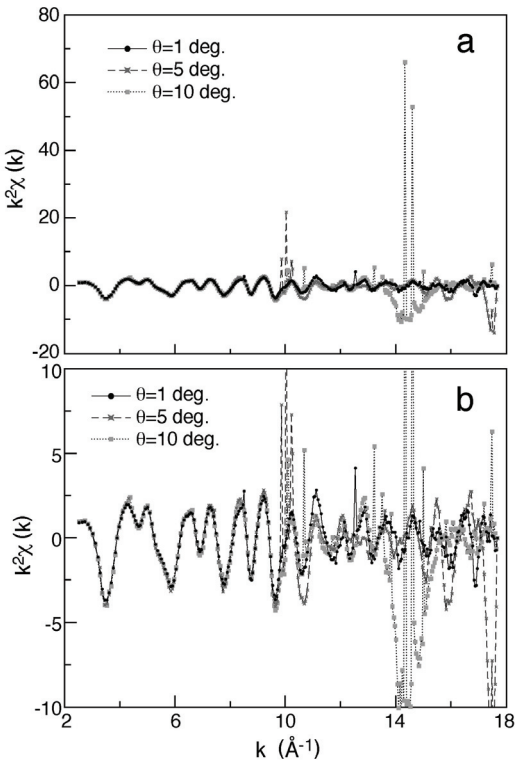

FIGURE 2. EXAFS osciilations of $(La,Sr)_2CuO_4$ thin film single crystal taken with various angle of incidence θ.

LOCAL STRUCTURE UNDER STRAIN

The crystal structure of LSCO is tetragonal at high temperatures where CuO_6 octahedra are connected to form a square-planar network sharing oxygen atoms. Each copper ion is surrounded with four in-plane oxygens (O_p) and two apical oxygens (O_{ap}). The CuO_6 octahedron is elongated along the *c*-axis resulting in two long (2.40 Å) and four short (1.89 Å) bonds by Jahn-Teller (JT) distortion. The lattice constant a_0 for LSCO/LSAO is 3.758 Å, smaller than that of optimally doped LSCO a_0 =3.778 Å by 0.02 Å or 0.5 %. Thus LSCO films grown on LSAO substrate are under compressive strain. Because of strain, the in-plane lattice is shortened while the out-of-plane lattice is expected to increase (the Poisson effect). In contrast, the lattice constant of LSCO/STO (a_0 =3.794 Å) is larger than that of LSCO by 0.016 Å or 0.4 %. The epilayers are under either tensile or compressive strain with almost the same magnitude of deformation of local lattice. Our results indicate that in both cases the local displacement of the CuO_6 octahedra is 0.01 Å or 0.5 %, in agreement with crystallographic lattice deformation.

The advantage of monitoring segmented solid angle using a PAD is obvious in the EXAFS data in Fig. 2. Fluorescence yield measurement in a surface-sensitive geometry is more reliable than monitoring secondary electron yield. Segmented monitoring solves the major problem in fluorescence yield, *i.e.*, interference of substrates. Detailed analysis of the NN contribution showed that the local lattice (oxygen displacement) undergoes unusual distortion at low temperature. The anomalous distortion indicates that the local lattice becomes inhomogeneous giving the short undistorted and long distorted Cu-O_p bonds.[2] As superfluid density (fraction of metallic domain) is known to linearly related to T_c, [7] the observed significant suppression of T_c is related to increased inhomogeneity [8].

SUMMARY

In this paper, we report that segmented x-ray detector is quite useful in fluorescence-detected XAS experiments on thin film single crystals. Fluorescence detection can probe entire region of thin films. However, the interference of substrates such as diffractions or x-ray standing waves have long been serious experimental problems. Monitoring spatial distribution of fluorescence x-ray by segmented detector such as PAD can find artifacts. By carefully adjusting two parameters, *i.e.*, angle of incidence and azimuthal orientation, artifacts due to substrates are completely removed.

The present electronics is capable of handling about 100 kHz count rate per channel. Use of digital electronics with a maximum count rate of 1 MHz per channel (under development) or the total count rate of 0.1 GHz. The advantage of PAD in packing density is clear but improved fabrication technology (See G. Foran *et al.*, this issue) provides energy resolution close to theoretical limit.

REFERENCES

1. J.G. Bednorz and K.A. Müller, *Z. Phys*. **B64**, 189 (1986).
2. A. Bianconi *et al*., *Phys. Rev. Lett.* **76**, 3412 (1996).
3. H. Oyanagi *et al.*, *J. Synchrotron Radiation* **13**, 314 (2006)
4. H. Oyanagi *et al*., *Nucl. Instrum. & Meth*., **A513**, 340 (2002).
5. H. Saito and M. Naito, *Physica C* **280**, 178 (1997).
6. J. Rehr, S.I. Zabrinsky, and R.C. Albers, *Phys. Rev. Lett*. **69**, 3397 (1992).
7. Y.J. Uemura, *et al*., *Phys. Rev. Lett*. **62**, 2317 (1989).
8. H. Oyanagi *et al*., *unpublished.*